

Analytical and numerical modeling of interfacial stresses in beams bonded with a thin plate

Tahar Hassaine Daouadji^{*1,2}

¹Département de génie civil, Université Ibn Khaldoun Tiaret; BP 78 Zaaroura, 14000 Tiaret, Algérie

²Laboratoire de Géomatique et Développement Durable, Université Ibn Khaldoun de Tiaret, Algérie

(Received September 17, 2016, Revised September 27, 2016, Accepted October 21, 2016)

Abstract. The composite plate to upgrade structures and, in particular, to extend the lives of reinforced concrete beams has wide applications. One of the main aspects of the bonded strengthening technology is the stress analysis of the reinforced structure. In particular, reliable evaluation of the adhesive shear stress and of the stress in the composite plates is mandatory in order to predict the beam's failure load. In this paper, a finite element analysis is presented to calculate the stresses in the reinforced beam under mechanical loads. The numerical results was compared with the analytical approach, and a parametric study was carried out to show how the maximum stresses have been influenced by the material and geometry parameters of the composite beam.

Keywords: finite element analysis; RC beam; interfacial stresses; strengthening; composite plate

1. Introduction

There are many cases where concrete structures need to be strengthened. Fiber reinforced polymer (FRP) composites, due to their high strength and corrosion resistance properties are widely applied in these cases. The composite plate to upgrade structures and, in particular, to extend the lives of reinforced concrete beams has wide applications. One of the main aspects of the bonded strengthening technology is the stress analysis of the reinforced structure. In particular, reliable evaluation of the adhesive shear stress and of the stress in the CFRP plates is mandatory in order to predict the beam's failure load. Recently, many authors conducted a numerical study on the static behaviour of RC beams strengthened with composites in different directions (Tounsi 2006, Benyoucef 2006, Tounsi *et al.* 2007, Roberts 1989, Hassaine Daouadji 2012, Rabahi *et al.* 2016 and 2015, Hassaine Daouadji *et al.* 2016, Hadji 2016, Smith and Teng 2001, Shen 2001, Yang 2007, Bouakaz 2014, El mahi 2014, Guenaneche 2014, Krour 2014, Touati 2015, Zidani 2015, Choi 2011, Kang 2012, Ramseyer 2012, Zhang 2016, Yang 2010). Numerical examples and a parametric study are presented to illustrate the governing parameters that control the stress concentrations at the edge of the FRP strip. Finally, the results of these investigations show that the interface bond-stresses are non-uniformly distributed along the reinforced boundaries. It is

*Corresponding author, Professor, E-mail: daouadjitah@yahoo.fr

believed that the present results will be of interest to civil and structural engineers and researchers.

The present work concerns the shear and normal stresses concentrations at the ends of the composite overlay (cut-off cross-sections). The objective of this study is to formulate a finite element model for studying such stresses; in particular, their distribution along the beam axis. The first numerical results presented in this paper are limited to the case of a composite laminate applied only to the bottom of a simply supported beam loaded in flexure, when the effects (non-uniform distribution along the strengthened boundaries) related to the out-of-plane warping of the cross-section are less relevant. In this paper, the details of the interfacial shear and normal stress are analyzed by the finite element method. The effects of the material and geometry parameters on the interface stresses are considered and compared with that resulting from literature. Finally, some concluding remarks are summarized in conclusion. It is believed that the present results will be of interest to civil and structural engineers and researchers.

2. Method of solution

2.1 Assumptions

The present analysis takes into consideration the transverse shear stress and strain in the beam and the plate but ignores the transverse normal stress in them. One of the analytical approach proposed by Hassaine Daouadji, Tounsi *et al.* (2012) for concrete beam strengthened with a bonded FRP Plate (Fig. 1) was used in order to compare it with a finite element analysis. The

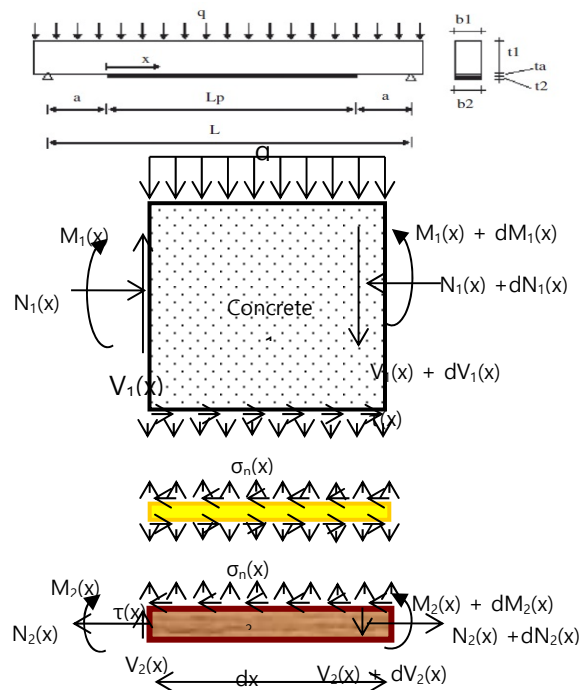


Fig. 1 Simply supported RC beam strengthened with bonded FRP plate

analytical approach (Hassaine Daouadji, Tounsi *et al.* 2012) is based on the following assumptions

1. Elastic stress strain relationship for concrete, composite and adhesive
2. There is a perfect bond between the composite plate and the beam
3. The adhesive is assumed to only play a role in transferring the stresses from the concrete to the composite plate reinforcement
4. The stresses in the adhesive layer do not change through the direction of the thickness.

Since the composite laminate is an orthotropic material, its material properties vary from layer to layer. In analytical study (Hassaine Daouadji, Tounsi *et al.* 2012), the laminate theory is used to determine the stress and strain behaviours of the externally bonded composite plate in order to investigate the whole mechanical performance of the composite - strengthened structure. The laminate theory is used to estimate the strain of the symmetrical composite plate.

2.2 Shear stress distribution along the FRP - concrete interface

The governing differential equation for the interfacial shear stress (Hassaine Daouadji, Tounsi *et al.* 2012) is expressed as

$$\frac{d^2 \tau(x)}{dx^2} - K_1 \left(A'_{11} + \frac{b_2}{E_1 A_1} + \frac{(y_1 + t_2/2)(y_1 + t_a + t_2/2)}{E_1 I_1 D'_{11} + b_2} b_2 D'_{11} \right) \tau(x) + K_1 \left(\frac{(y_1 + t_2/2)}{E_1 I_1 D'_{11} + b_2} D'_{11} \right) V_T(x) = 0 \quad (1)$$

Where

$$K_1 = \frac{1}{\left(\frac{t_a}{G_a} + \frac{t_1}{4 G_1} \right)} \quad (2)$$

For simplicity, the general solutions presented below are limited to loading which is either concentrated or uniformly distributed over part or the whole span of the beam, or both. For such loading, $d^2 V_T(x)/dx^2=0$, and the general solution to Eq. (1) is given by

$$\tau(x) = B_1 \cosh(\lambda x) + B_2 \sinh(\lambda x) + m_1 V_T(x) \quad (3)$$

Where

$$\lambda^2 = K_1 \left(A'_{11} + \frac{b_2}{E_1 A_1} + \frac{(y_1 + t_2/2)(y_1 + t_a + t_2/2)}{E_1 I_1 D'_{11} + b_2} b_2 D'_{11} \right) \quad (4)$$

And

$$m_1 = \frac{K_1}{\lambda^2} \left(\frac{(y_1 + t_2/2)}{E_1 I_1 D'_{11} + b_2} D'_{11} \right) \quad (5)$$

And B_1 and B_2 are constant coefficients determined from the boundary conditions. In the present study, a simply supported beam has been investigated which is subjected to a uniformly distributed load (Fig. 1). The interfacial shear stress for this uniformly distributed load at any point is written as (Hassaine Daouadji, Tounsi *et al.* 2012)

$$\tau(x) = \left[\frac{m_2 a}{2} (L - a) - m_1 \right] \frac{q e^{-\lambda x}}{\lambda} + m_1 q \left(\frac{L}{2} - a - x \right) \quad 0 \leq x \leq L_p \quad (6)$$

Where q is the uniformly distributed load and x ; a ; L and L_p are defined in Fig. 1.

2.3 Normal stress distribution along the FRP - concrete interface

The following governing differential equation for the interfacial normal stress (Hassaine Daouadji, Tounsi *et al.* 2012).

$$\frac{d^4 \sigma_n(x)}{dx^4} + K_n \left(D_{11}' + \frac{b_2}{E_1 I_1} \right) \sigma_n(x) - K_n \left(D_{11}' \frac{t_2}{2} - \frac{y_1 b_2}{E_1 I_1} \right) \frac{d\tau(x)}{dx} + \frac{q K_n}{E_1 I_1} = 0 \quad (7)$$

The general solution to this fourth-order differential equation is

$$\sigma_n(x) = e^{-\beta x} [C_1 \cos(\beta x) + C_2 \sin(\beta x)] + e^{\beta x} [C_3 \cos(\beta x) + C_4 \sin(\beta x)] - n_1 \frac{d\tau(x)}{dx} - n_2 q \quad (8)$$

For large values of x it is assumed that the normal stress approaches zero and, as a result, $C_3=C_4=0$. The general solution therefore becomes

$$\sigma_n(x) = e^{-\beta x} [C_1 \cos(\beta x) + C_2 \sin(\beta x)] - n_1 \frac{d\tau(x)}{dx} - n_2 q \quad (9)$$

Where

$$\beta = \sqrt[4]{\frac{K_n}{4} \left(D_{11}' + \frac{b_2}{E_1 I_1} \right)} \quad (10)$$

$$n_1 = \left(\frac{y_1 b_2 - D_{11}' E_1 I_1 t_2 / 2}{D_{11}' E_1 I_1 + b_2} \right) \quad n_2 = \frac{1}{D_{11}' E_1 I_1 + b_2} \quad (11)$$

As is described by Hassaine Daouadji, Tounsi *et al.* (2012), the constants C_1 and C_2 in Eq. (9) are determined using the appropriate boundary conditions and they are written as follows

$$C_1 = \frac{K_n}{2 \beta^3 E_1 I_1} [V_T(0) + \beta M_T(0)] - \frac{n_3}{2 \beta^3} \tau(0) + \frac{n_1}{2 \beta^3} \left(\frac{d^4 \tau(0)}{dx^4} + \beta \frac{d^3 \tau(0)}{dx^3} \right) \quad (12)$$

$$C_2 = - \frac{K_n}{2 \beta^2 E_1 I_1} M_T(0) - \frac{n_1}{2 \beta^2} \frac{d^3 \tau(0)}{dx^3} \quad (13)$$

$$n_3 = b_2 K_n \left(\frac{y_1}{E_1 I_1} - \frac{D_{11}' t_2}{2 b_2} \right) \quad (14)$$

The above expressions for the constants C_1 and C_2 has been left in terms of the bending moment $M_T(0)$ and shear force $V_T(0)$ at the end of the soffit plate. With the constants C_1 and C_2 determined, the interfacial normal stress can then be found using Eq. (9)

2.4 Finite element analysis

In comparison with laboratory tests which are highly time and cost demanding, the numerical

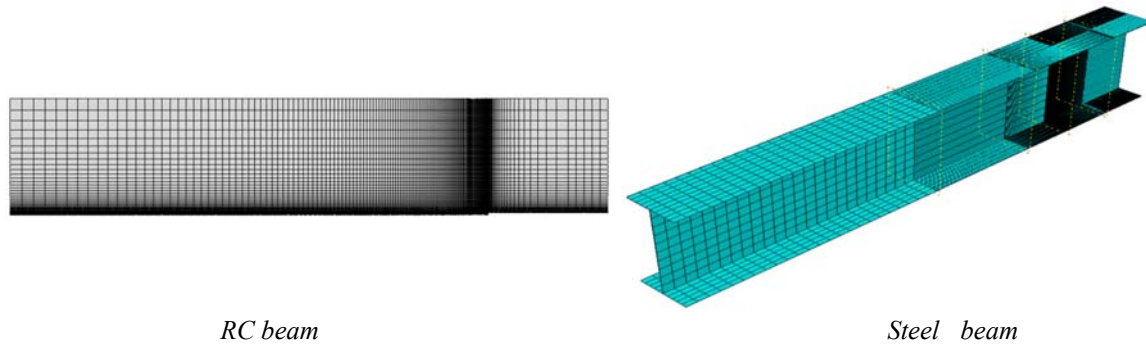


Fig. 2 Finite Element mesh of a half hybrid beam strengthened with bonded composite plate model

simulation is cheaper, time-saving, not so dangerous and more information. As the computational power has intensely increased, numerical methods, in particular the finite element method (FEM), have also been resorted for analysis of many practical engineering problems. The modeling process in Abaqus (2007) consists of defining the various components of the model individually i.e., the reinforced RC beam (and steel I-beam), FRP plate and adhesive layer were defined as parts, each compatible with the other so as to provide a complete analysis. The modeling itself is an iterative process, in that it takes several analyses to be able to simulate a particular set of characteristics effectively. A 4-node linear quadrilateral, type S4R was established, in which only one half of the beam was considered because of symmetry geometry and loading of the beam (Fig. 2). All nodes at mid-span were restrained to produce the required symmetry, and nodes at the end of the RC beam and steel I-beam were restrained to represent simply roll-supported conditions. The finite element mesh was refined in correspondence of the reinforcement ends in order to capture the relevant stress concentration with a total of C3D20R-131150 elements for FRP- RC hybrid beam and 23730 elements and 24552 nodes for steel I-beam. The number of elements used depends largely on the geometric parameters such as the length and the cross-sectional perimeter. In order to obtain accurate stress results at the ends of the plate, a fine mesh was deployed in these areas, as shown in Fig. 2. The relevant geometrical and mechanical properties used in the finite element analysis were the same as that used in the analytical method shown in Table 2. To simulate correctly the interaction behavior between the various components of the composite beams, a surface-to-surface contact interaction describes contact between two deformable surfaces. Element types and material properties were then specified and assigned to each corresponding part. A single concentrated load was applied at the mid-span of the strengthened beam. While the beam was assigned isotropic material properties, unidirectional laminate stress-strain relationship was adopted for the FRP plate and elastic material properties for the adhesive layer. In this work, the stresses have been obtained from the average values of the stress in the bottom elements of the adhesive layer.

3. Numerical verification and discussions

The present analytical solution is verified in this section by comparing its predictions with experimental results obtained by Jones, Swamy *et al.* (1988), with analytical solutions by Smith and Teng (2001), Tounsi (2007), Yang and Wu (2007) and Hassaine Daouadji, Tounsi *et al.*

Table 1 Dimensions and material properties

Concrete	$b_1=155$ mm	$t_1=255$ mm	$E_1=31$ MPa	
Steel	$b_2=125$ mm	$t_1=6$ mm	$E_2=200\,000$ MPa	
Adhesive	$b_a=123$ mm	$t_a=1,5$ mm	$E_a=280$ MPa	$G_a=108$ MPa

Table 2 Geometric and material properties

Component	Width (mm)	Depth (mm)	Young's modulus (MPa)	Poisson's ratio	Shear modulus (MPa)
RC beam	$b_1=200$	$t_1=300$	$E_1=30\,000$	0.18	-
Adhesive layer RC beam	$b_a=200$	$t_a=4$	$E_a=3000$	0.35	-
GFRP plate (bonded RC beam)	$b_2=200$	$t_2=4$	$E_2=0\,000$	0.28	$G_{12}=5000$
GFRP plate (bonded steel beam)	$b_1=150$	$t_2=2$	$E_2=50\,000$	0.28	$G_{12}=5000$
GFRP plate (bonded Aluminium beam)	$b_2=20$	$t_2=2$	$E_2=50\,000$	0.28	$G_{12}=5000$
CFRP plate (bonded RC beam)	$b_2=200$	$t_2=4$	$E_2=140\,000$	0.28	$G_{12}=5000$
CFRP plate (bonded steel beam)	$b_1=150$	$t_2=2$	$E_2=140\,000$	0.28	$G_{12}=5000$
CFRP plate (bonded Aluminium beam)	$b_2=20$	$t_2=2$	$E_2=140\,000$	0.28	$G_{12}=5000$
Steel plate (bonded RC beam)	$b_2=200$	$t_2=4$	$E_2=200\,000$	0.3	-
Aluminium plate (bonded RC beam)	$b_2=200$	$t_2=4$	$E_2=65\,300$	0.3	
Aluminium beam (wall thickness 2 mm)	$b_1=20$	$t_2=30$	$E_2=65\,300$	0.3	
Adhesive layer (Aluminium beam)	$b_2=20$	$t_2=2$	$E_2=2\,000$	0.35	
Steel I- beam (IPE300)	$b_1=150$	$t_1=300$	$E_2=200\,000$	0.3	

(2012) and Finite element results conducted using ABAQUS (2007) for the same example beam subjected to UDL. For finite element analyses, due to the structural and loading symmetry of the beam, only one half span of the beam was analysed with appropriate boundary conditions imposed at the mid-span. The beam was modelled as a plane stress problem. A convergence study of the FE mesh was conducted, and only the converged results from a very fine mesh similar to that shown in Fig. 5 are presented in this paper.

3.1 Comparison of predictions with experimental data

The predicted stresses by the present theory have been compared to those of experimental results obtained by Jones *et al.* (1988). The geometry and materials properties of the specimen are summarized in Table 1. As it can be seen from Fig. 3 the predicted theoretical results agree with the experimental results presented by Jones *et al.* (1988). The interfacial shear stress distributions in the beam bonded with a soffit steel plate under the applied load 180 kN, are compared between the experimental results and those obtained by the present model. As it can be seen from Fig. 3, the predicted analytical results are in reasonable agreement with the experimental results.

3.2 Comparison with approximate solutions

The present simple solution is compared, in this section, with some approximate solutions

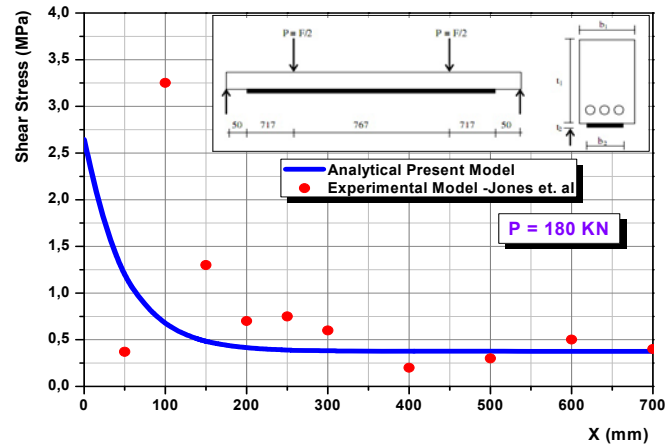


Fig. 3 Comparison of interfacial shear of the steel plated RC beam with the experimental results

available in the literature. These include Smith and Teng (2001), Tounsi (2007), Yang and Wu (2007) and Hassaine Daouadji, Tounsi *et al.* (2012) solutions uniformly distributed loads. A comparison of the interfacial shear and normal stresses from the different existing closed - form solutions and the present solution is undertaken in this section. An undamaged beams bonded with GFRP, CFRP, Steel and Aluminium plate soffit plate is considered. The beam is simply supported and subjected to a uniformly distributed load. A summary of the geometric and material properties is given in Table 2. The results of the peak interfacial shear and normal stresses are given in Table 3 for the beams strengthened by bonding GFRP, CFRP, Steel and Aluminium plate. As it can be seen from the results, the peak interfacial stresses assessed by the present theory are smaller compared to those given by Smith and Teng (2001), Tounsi (2007), Yang and Wu (2007) and Hassaine Daouadji, Tounsi *et al.* (2012) solutions. This implies that adherend shear deformation is an important factor influencing the adhesive interfacial stresses distribution. Fig. 4 plots the interfacial shear and normal stresses near the plate end for the example RC beam bonded with a CFRP plate for the uniformly distributed load case. Overall, the predictions of the different solutions agree closely with each other. The interfacial normal stress is seen to change sign at a short distance away from the plate end. The present analysis gives lower maximum interfacial shear and normal stresses than those predicted by Tounsi (2006) and Hassaine Daouadji, Tounsi *et al.* (2012), indicating that the inclusion of adherend shear deformation effect in the beam and soffit plate leads to lower values of σ_{\max} and σ_{\max} . However, the maximum interfacial shear and normal stresses given by Tounsi (2006) and Hassaine Daouadji, Tounsi *et al.* (2012) methods are lower than the results computed by the present solution. This difference is due to the assumption used in the present theory which is in agreement with the beam theory. Hence, it is apparent that the adherend shear deformation reduces the interfacial stresses concentration and thus renders the adhesive shear distribution more uniform. The interfacial normal stress is seen to change sign at a short distance away from the plate end.

The results of the peak interfacial shear and normal stresses are given in Table 3 for the RC beam with a GFRP, CFRP, Steel and Aluminum soffit plate. Table 3 shows that, for the UDL case, the present solution gives results which generally agree better with those from Smith and Teng (2001), Yang and Wu (2007), Tounsi (2007) and Hassaine Daouadji, Tounsi *et al.* (2012)

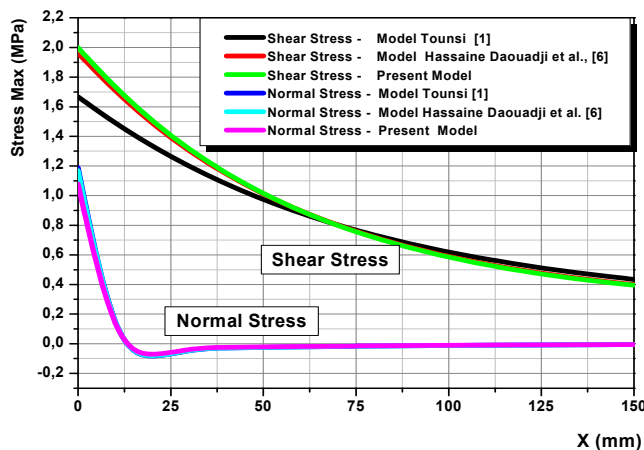


Fig. 4 Comparison of interfacial shear and normal stress for CFRP-plated RC beam with the analytical results

Table 3 Comparison of peak interfacial shear and normal stresses (MPa): Uniformly Distributed Load- UDL

Reinforced Concrete Beam bonded with a thin plate subjected to a uniformly distributed load								
Model	RC beam with CFRP plate		RC beam with GFRP plate		RC beam with steel plate		RC beam with aluminum plate	
	Shear	Normal	Shear	Normal	Shear	Normal	Shear	Normal
Present Model	1.998	1.188	1.121	0.913	2.340	1.282	1.439	1.002
Tounsi <i>et al.</i> (2007)	1.968	1.169	1.194	0.899	2.304	1.261	1.417	0.985
Smith and Teng (2001)	2.740	1.484	1.975	1.244	3.696	1.713	1.973	1.251
Hassaine Daouadji <i>et al.</i> (2012)	1.962	1.162	1.108	0.893	2.297	1.253	1.413	0.980
Yang and Wu (2007)	2.168	1.225	1.255	1.112	2.539	1.321	1.561	1.033
Steel Beam bonded with a thin plate subjected to a uniformly distributed load								
Model	Steel beam with CFRP plate		Steel beam with GFRP plate		Steel beam with steel plate		Steel beam with aluminum plate	
	Shear Stress	Normal Stress	Shear Stress	Normal Stress	Shear Stress	Normal Stress	Shear Stress	Normal Stress
Present Model	2.385	1.355	1.477	1.055				
Tounsi <i>et al.</i> (2007)	2.349	1.332	1.454	1.037				
Smith and Teng (2001)	2.580	1.397	1.597	1.087				
Hassaine Daouadji <i>et al.</i> (2012)	2.342	1.325	1.459	1.031				
Yang and Wu (2007)	3.270	1.691	2.025	1.316				
Aluminium Beam bonded with a thin plate subjected to a uniformly distributed load								
Model	Aluminium beam with CFRP plate		Aluminium beam with GFRP plate		Aluminium beam with steel plate		Aluminium beam with aluminum plate	
	Shear Stress	Normal Stress	Shear Stress	Normal Stress	Shear Stress	Normal Stress	Shear Stress	Normal Stress
Present Model	1.610	0.889	0.903	0.683				
Tounsi <i>et al.</i> (2007)	1.586	0.875	0.962	0.672				
Smith and Teng (2001)	1.748	0.917	0.987	0.832				
Hassaine Daouadji <i>et al.</i> (2012)	1.580	0.869	0.891	0.667				
Yang and Wu (2007)	2.091	1.081	1.172	0.980				

solutions. The latter two again give similar results. In short, it may be concluded that all solutions are satisfactory for RC beams bonded with a thin plate as the rigidity of the soffit plate is small in comparison with the that of the RC beam. Those solutions which consider the additional bending and shear deformations in the soffit plate due to the interfacial shear stresses give more accurate results. The present solution is the only solution which covers the uniformly distributed loads and considers this effect and the effects of other parameters.

3.3 Comparison with numerical model

Finite element results conducted using ABAQUS (2007) for the same example beam subjected to UDL. For finite element analyses, due to the structural and loading symmetry of the beam, only one half span of the beam was analysed with appropriate boundary conditions imposed at the mid-span. The beam was modelled as a plane stress problem. A convergence study of the FE mesh was conducted, and only the converged results from a very fine mesh similar to that shown in Fig. 5 are presented in this paper. The present solution is again in close agreement with the FE results except a small region near the plate end. The shear stresses at the PA and AB interfaces predicted by the FE method are very large at the plate end and do not reduce to zero. One of advantages of FEM simulation is that the detailed distributions of the normal and shear stresses along the interfaces can be produced. A simply supported RC beam strengthened with a bonded composite plate. Taking advantage of the symmetry of the specimens, only one quarter of the beams was modelled, The influence of the mesh size on the predicted shear stress at the cut-off points was noticeable. In general, increasing the size of the elements results in a proportional increase in the distances among the integration points within the element. Therefore, the induced shear stresses at the strip cut-off points are averaged over a large distance and are considerably less than the true values. Decreasing the size of the elements results in a substantial increase in the maximum shear stress up to a certain limit beyond which no further increase in the shear stresses is observed. The size of the elements at this transition stage is termed the optimum size. The optimum size of the elements in the longitudinal as well as in the vertical directions was determined as shown in Fig. 5. Further refinement of the mesh around the cutoff points increased the predicted shear stress by less than 0.5percent. The final mesh dimensions used for 92000 elements (mesh 4). The FEM solutions are

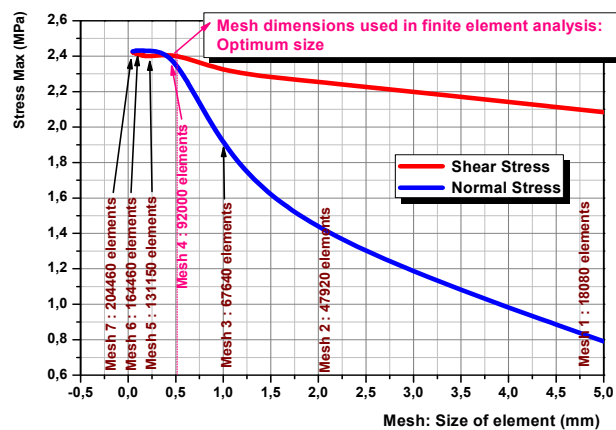


Fig. 5 Influence of element size in the direction on maximum shear and normal stress at cutoff point

compared with the present analytical model and the interfacial shear and normal stress distributions near the end of FRP are shown in Figs. 6, 7 and 8. The FEM results are in reasonable agreement with the analytical results.

3.4 Parametric studies

The effects of geometrical and material properties on the interfacial stresses in a plated RC beam subjected to UDL loads are examined in this section. The parametric study program was based on FE analysis work and analytically approach, which will help engineers in optimizing their design parameters, the effects of several parameters were investigated. The material used for the present studies is an RC beam bonded with a glass or carbon fibre reinforced plastic (GFRP or CFRP) or with a steel plate. The beams are simply supported and subjected to a uniformly distributed load. A summary of the geometric and material properties is given in Table 2. From results presented in Figs. 6 and 7 gives interfacial normal and shear stresses for the RC beam

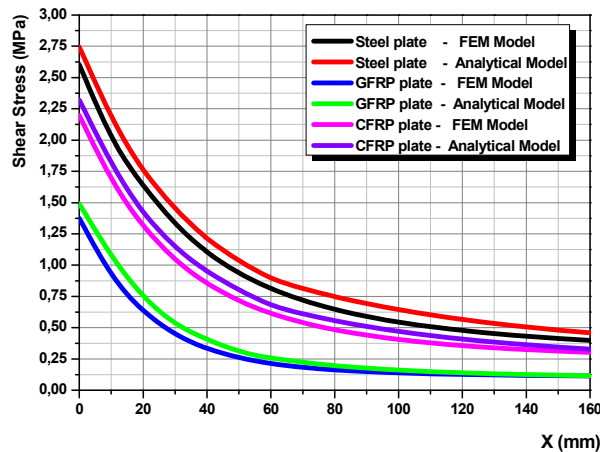


Fig. 6 Effect of plate stiffness on interfacial shear stresses in strengthened beam

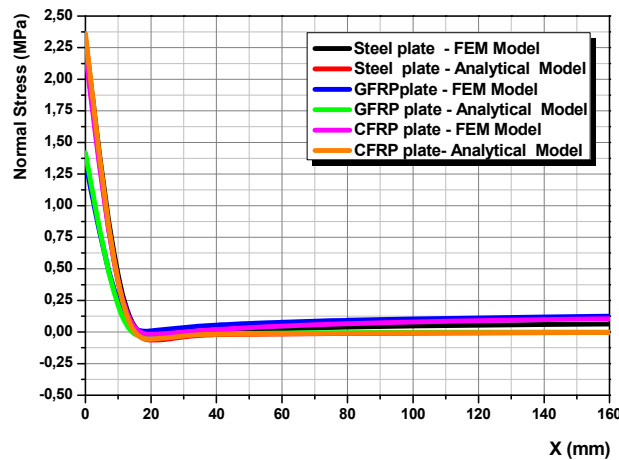


Fig. 7 Effect of plate stiffness on interfacial normal stresses in strengthened beam

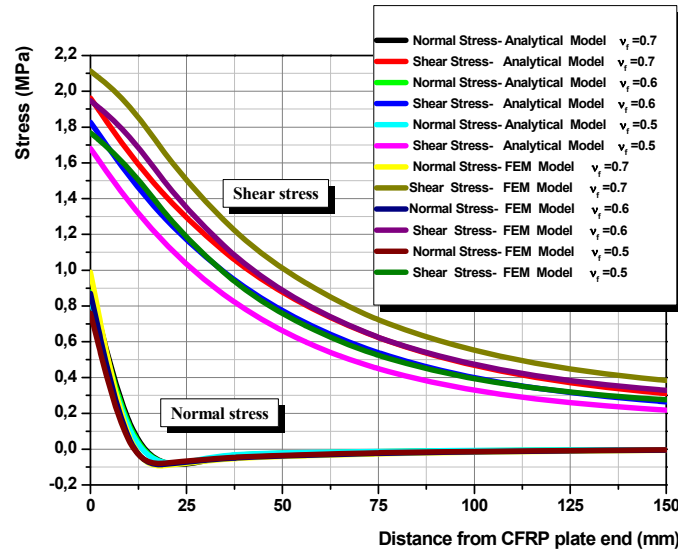


Fig. 8 Effect of fiber volume fraction on interfacial stresses in RC beam strengthened with CFRP

bonded with a steel plate, CFRP plate and GFRP plate, respectively, which demonstrates the effect of plate material properties on interfacial stresses. The results show that, as the plate material becomes softer (from steel to CFRP and then GFRP), the interfacial stresses become smaller, as expected. This is because, under the same load, the tensile force developed in the plate is smaller, which leads to reduced interfacial stresses. The position of the peak interfacial shear stress moves closer to the free edge as the plate becomes less stiff. Fig. 8 show, the effect of fiber volume fractions V_f ($=0.5, 0.6$ and 0.7) on the variation of shear and normal adhesive stresses. It can be seen that the interfacial shear stresses are reduced with decreases in fiber volume fraction. However, almost no effect is observed on the variation of interfacial normal stresses.

4. Conclusions

This paper has been concerned with the prediction of interfacial shear and normal stresses in beams strengthened by an externally bonded plate. Such interfacial stresses provide the basis for understanding debonding failures in such beams and for the development of suitable design rules. The interfacial stresses in the FRP-RC hybrid beam were investigated by analytical and the finite element method and subjected to a uniformly distributed bending load. The analytical analysis include the consideration of the adherend shear deformations by assuming a parabolic shear stress through the thickness of both the concrete beam and bonded plate. The solution methodology is general in nature and may be applicable to the analysis of other types of composite structures. By comparing with experimental and numerical results, this present solution provides satisfactory predictions to the interfacial stress in the plated beams. The numerical examples show that the FE calculations are in good agreements with the theoretical analysis. Observations were made based on the numerical results concerning their possible implications to practical designs. It can be concluded that this research is helpful for the understanding on mechanical behavior of the

interface and design of the FRP-RC hybrid structures. The new solution is general in nature and may be applicable to all kinds of materials.

Acknowledgments

The authors thank the referees for their valuable comments.

References

- Abaqus guide Version 6.7 (2007), "Computer software for interactive finite element analysis by Hibbit", Karlsson & Sorensen, Inc. Pawtucket, RI.
- Benyoucef, S., Tounsi, A., Meftah, S.A. and Adda Bedia, E.A. (2006), "Approximate analysis of the interfacial stress concentrations in FRP-RC hybrid beams", *Compos. Interface.*, **13**(7), 561-571.
- Bouakaz, K., Hassaine Daouadji, T., Meftah, S.A., Ameer, M. and Adda Bedia, E.A. (2014), "A numerical analysis of steel beams strengthened with composite materials", *Mech. Compos.Mater.*, **50**(4), 685-696.
- Choi, D.U., Kang, T.H.K., Ha, S.S., Kim, K.H. and Kim, W. (2011), "Flexural and bond behavior of concrete beams strengthened with hybrid carbon-glass fiber-reinforced polymer sheets", *ACI Struct. J.*, **180**(1), 90-98.
- El Mahi Benrahou, K.H., Belakhdar, K., Tounsi, A. and Adda Bedia, E.A. (2014), "Effect of the tapered of the end of a FRP plate on the interfacial stresses in a strengthened beam used in civil engineering applications", *Mech. Compos. Mater.*, **50**(4), 465-474.
- Guenaneche, B., Tounsi, A. and Adda Bedia, E.A. (2014), "Effect of shear deformation on interfacial stress analysis in plated beams under arbitrary loading", *Adhesion & Adhesives*, **48**, 1-13.
- Kang, T.H.K., Howell, J., Kim, S. and Lee, D.J. (2012), "A State-of-the-art review on debonding failures of FRP laminates externally adhered to concrete", *Int. J. Concrete Struct. Mater.*, **6**(2), 123-134.
- Krou, B., Bernard, F. and Tounsi, A. (2014), "Fibers orientation optimization for concrete beam strengthened with a CFRP bonded plate: A coupled analytical-numerical investigation", *Eng. Struct.*, **56**, 218-227.
- Hadji, L., Hassaine daouadji, T., Ait Amar Meziane, M., Tlidji, Y. and Adda Bedia, E.A. (2016), "Analyse of the interfacial stress in reinforced concrete beams strengthened with externally bonded CFRP plate", *Steel Compos. Struct.*, **20**(2), 413-429.
- Hassaine Daouadji, T., Tounsi, A. and Adda bedia, E.A. (2012), "Analyse des contraintes d'interface dans les poutres en béton armé renforcées par collage des stratifiées composites", *Revue de génie industriel*, **8**, 3-12.
- Hassaine Daouadji, T., Hadji, L., Ait Amar Meziane, M. and Bekki, H. (2016), "Elastic analysis effect of adhesive layer characteristics in steel beam strengthened with a fiber-reinforced polymer plates", *Struct. Eng. Mech.*, **59**(1), 83-100.
- Yang, J., Ye, J. and Niu, Z. (2007), "Interfacial shear stress in FRP-plated RC beams under symmetric loads", *Cement Concrete Compos.*, **29**(5), 421-432.
- Yang, J. and Ye, J. (2010), "An improved closed-form solution to interfacial stresses in plated beams using a two-stage approach", *Int. J. Mech. Sci.*, **52**(1), 13-30.
- Jones, R., Swamy, R.N. and Charif, A. (1988), "Plate separation and anchorage of reinforced concrete beams strengthened by epoxy-bonded steel plates", *Struct. Eng.*, **66**(5), 85-94.
- Rabahi, A., Adim, B., Chergui, S. and Hassaine Daouadji, T. (2015), "Interfacial stresses in FRP-plated RC beams: Effect of adherend shear deformations", *Multiphys. Model. Simulat. Syst. Des. Monit. Appl. Condition Monit.*, **2**, 317-326.
- Rabahi, A., Hassaine Daouadji, T., Abbes, B. and Adim, B. (2016), "Analytical and numerical solution of the interfacial stress in reinforced-concrete beams reinforced with bonded prestressed composite plate", *J.*

- Reinforce. Plast. Compos.*, **35**(3), 258-272.
- Ramseyer, C. and Kang, T.H.K. (2012), "Post-damage repair of prestressed concrete girders", *Int. J. Concrete Struct. Mater.*, **6**(3), 199-207.
- Roberts, T.M. (1989), "Approximate analysis of shear and normal stress concentrations in the adhesive layer of plated RC beams", *Struct. Eng.*, **67**(12), 229-233.
- Shen, H.S., Teng, J.G. and Yang, J. (2001), "Interfacial stresses in beams and slabs bonded with thin plate", *J. Eng. Mech.*, ASCE, **127**(4), 399-406.
- Smith, S.T. and Teng, J.G. (2001), "Interfacial stresses in plated beams", *Eng. Struct.*, **23**(7), 857-871.
- Touati, M., Tounsi, A. and Benguediab, M. (2015), "Effect of shear deformation on adhesive stresses in plated concrete beams: Analytical solutions", *Comput. Concrete*, **15**(3), 141-166.
- Tounsi, A. (2006), "Improved theoretical solution for interfacial stresses in concrete beams strengthened with FRP plate", *Int. J. Solid. Struct.*, **43**(14), 4154-4174.
- Tounsi, A. and Benyoucef, S. (2007), "Interfacial stresses in externally FRP-plated concrete beams", *Int. J. Adhes Adhes*, **27**(3), 207-215.
- Tounsi, A., Hassaine Daouadji, T., Benyoucef, S. and Adda bedia, E.A. (2009), "Interfacial stresses in FRP-plated RC beams: Effect of adherend shear deformations", *Int. J. adhesion and adhesives*, **29**(4), 313-351.
- Zidani, M.B., Belakhdar, K., Tounsi, A. and Adda Bedia, E.A. (2015), "Finite element analysis of initially damaged beams repaired with FRP plates", *Compos. Struct.*, **134**, 429-439.
- Yang, J. and Wu, Y.F. (2007), "Interfacial stresses of FRP strengthened concrete beams: Effect of shear deformation", *Compos. Struct.*, **80**(3), 343-351.
- Zhang, X., Zhu, D., Yao, Y., Zhang, H. and Mobasher, B. (2016), "Experimental study of tensile behaviour of AFRP under different strain rates and temperatures", *Struct. Integrity Maint.*, **1**(1), 22-34.